

How to predict the future face? A 3D methodology to forecast the aspect of patients after orthognathic surgeries

Original

How to predict the future face? A 3D methodology to forecast the aspect of patients after orthognathic surgeries / Olivetti, E.C., Marcolin, F., Moos, S., Vezzetti, E., Borbon, C., Zavattero, E., Ramieri, G.. - In: COMPUTER METHODS AND PROGRAMS IN BIOMEDICINE. - ISSN 1872-7565. - 265:(2025). [10.1016/j.cmpb.2025.108757]

Availability:

This version is available at: 11583/3001378 since: 2025-06-30T10:42:58Z

Publisher:

Elsevier Ireland Ltd

Published

DOI:10.1016/j.cmpb.2025.108757

Terms of use:

This article is made available under terms and conditions as specified in the corresponding bibliographic description in the repository

Publisher copyright

(Article begins on next page)



Contents lists available at ScienceDirect

Computer Methods and Programs in Biomedicine

journal homepage: www.sciencedirect.com/journal/computer-methods-and-programs-in-biomedicine



How to predict the future face? A 3D methodology to forecast the aspect of patients after orthognathic surgeries

Elena Carlotta Olivetti^{a,*}, Federica Marcolin^a, Sandro Moos^a, Enrico Vezzetti^a,
Claudia Borbon^b, Emanuele Zavattero^b, Guglielmo Ramieri^b

^a Department of Management and Production Engineering, Politecnico di Torino, corso Duca degli Abruzzi 24, 10129 Torino, Italy

^b Department of Surgical Sciences, Division of Maxillofacial Surgery, University of Turin, Città della Salute e della Scienza Hospital, 10129 Torino, Italy

ARTICLE INFO

Keywords:

Dental malocclusion
Orthognathic surgery
Soft tissue displacement
3D soft tissue prediction
Displacement vectorial map

ABSTRACT

Background and objective: Despite the availability of several commercial solutions for predicting the soft tissue outcomes of maxillofacial surgeries, none have proven sufficiently reliable for routine clinical use. This study proposes a 3D methodology for predicting soft tissue displacement following maxillofacial surgery without relying on mechanical modeling, unlike most existing approaches.

Methods: Pre- and post-operative Cone Beam Computed Tomography scans of patients with class III malocclusion were collected. Tailored image processing and volume reconstruction techniques were applied to semi-automatically generate 3D soft tissue models. Cephalometric landmarks were identified to perform a geometrical similarity analysis among patients with the same malocclusion class undergoing the same surgical procedure. Vectorial displacement maps were generated to capture the soft tissue changes from pre- to post-operative and were then applied to the pre-operative of test patients to predict soft tissue outcomes. Euclidean distances were calculated between predicted and real post-operative positions, and the Wilcoxon signed-rank test was conducted to assess statistical differences between predicted and real landmark coordinates.

Results: Error maps indicated that approximately 70 % of predicted facial points had errors below 2.5 mm, while around 10 % ranged between 2.5 mm and 3 mm. Statistically significant differences ($p < 0.05$) were observed only for the gonion and cheilion.

Conclusion: The findings support the validity of the geometrical similarity analysis and the vectorial displacement map approach. The simplicity and promising accuracy of the proposed method encourage further investigations across different surgical procedures. Additionally, integrating this methodology into surgical planning could offer a viable alternative to commercial solutions. This low-cost, computationally efficient prediction method is designed to improve as more patient data become available. The proposed method is patent pending.

1. Introduction

Persons affected by severe dental malocclusion must face against several problems, from the most obvious to those less predictable. The mouth is the most affected by these dysmorphisms causing chewing difficulties, jaw pain, crowding of teeth and consequently susceptibility to developing caries, tendencies to breathe through the mouth with dryness of mouth and throat. The misalignment of the superior and inferior dental arches forces the maxilla and the mandible to an abnormal work with irregular loads that have negative repercussions at the temporomandibular level: neck pain, headaches and ear buzzing are

possible undesirable consequences. In addition to these already unpleasant aspects, a correlation with postural problems was suggested [1, 2], although no clearly supporting findings emerged from the literature [3–5]. Obviously, the aesthetical aspect is severely influenced by maxillo-mandibular malocclusion; asymmetry, lack of harmonious balance, flat cheekbones make the face unattractive, with social and relational consequences [6–10]. Malocclusion can fall into three different classes: class I occurs when the upper dental arch slightly overlaps the lower dental arch, class II (commonly known as retrognathism) occurs when the upper arch greatly overlaps the lower one, causing dysfunctionality of the bite, and finally class III (also known as prognathism)

* Corresponding author.

E-mail address: elena.olivetti@polito.it (E.C. Olivetti).

<https://doi.org/10.1016/j.cmpb.2025.108757>

Received 6 November 2024; Received in revised form 9 March 2025; Accepted 28 March 2025

Available online 7 April 2025

0169-2607/© 2025 The Authors. Published by Elsevier B.V. This is an open access article under the CC BY-NC-ND license (<http://creativecommons.org/licenses/by-nc-nd/4.0/>).

occurs when the lower arch protrudes forward the upper arch. This last is the most critical malocclusion and the one that can result in the most severe aesthetic and functional problems. In this last case, surgical treatment is often necessary. These dentofacial deformities are commonly treated with combined orthodontic and surgical interventions, particularly Le Fort I osteotomy, bilateral sagittal split osteotomy, intraoral ramus vertical osteotomy, sagittal split ramus osteotomy, bimaxillary surgery and genioplasty [11,12]. Additionally, zygomatic valgization can be performed in presence of maxillary hypoplasia to reach facial balance. Consequently, the definition of proper functionality, although a priority, cannot be dissociated from the achievement of a harmonious and aesthetically more pleasing appearance [13].

Commonly, interventions have been planned by means of bi-dimensional (2D) approaches, able to help surgeons in planning the operations but not eligible to realistically give an idea of the real aesthetic result [12]. As the other branches of medicine and surgery, orthognathic and maxillofacial surgery benefits from the advances in medical imaging technology, enabling three-dimensional (3D) technologies for surgical planning and simulation for both hard and soft tissue. Focusing on the soft tissue simulation, and consequently on the prediction of the aesthetic result, the spreading of 3D solutions finds fertile ground in the drive toward greater interaction between patient and surgical team, where more effective communication leads to patient involvement in the planning [14,15]. Nevertheless, practitioners are always very cautious in presenting to the patient the simulation of future facial appearance. This is due to the fact that, particularly among the 3D solutions, none seems to reach a level of reliability adequate to the purpose [12–16], presenting a plausible more than the real facial aspect. The general lack of accuracy highlighted for some of the most widespread 3D prediction software [12–16] could be detrimental for the patient–surgeon interaction, as the unreliable aesthetic prediction could raise unrealistic expectations [14]. Modabber et al. investigated the abilities of ProPlan CMF (Materialise NV, Leuven, Belgium) and Dolphin Imaging (Dolphin & Management Solution, Chatsworth, California, USA), to predict the soft tissue aspect; they found that relevantly different results were obtained for the same patient, suggesting a critical view on the effective benefits of soft tissue prediction [17]. A conflicting conclusion was found by Lee et al. [18], that affirmed that ProPlan CMF produced clinically satisfactory soft tissue predictions; however, only one type of intervention was considered in this case.

Along with 3D commercial solutions for the forecasting of the soft tissue facial modifications after surgeries, whose advantages and criticalities have been discussed in several works [12–19], other solutions have been proposed in the recent years. To reduce the long computation of the complex models and the tedious meshes preparation involved in commercial soft tissue simulation programs, Alcañiz et al. [20] proposed a FEM implementation with a non-linear Neo-Hookean material; thus, they suggested that non-linearity and heterogeneity are not fundamental in the prediction, except for specific areas such as the lips. Although the good result, the method seemed apt to some surgical procedures more than others.

Similarly to other research fields, machine learning and deep learning are emerging as revolutionary tools in orthognathic and maxillofacial surgery. This is proven by the number of studies proposed in the literature; to this regard, recent analysis of the literature have been conducted to the aim of offering a clear overview of the actual state-of-the-art (sota) [21–25]. From these reviews, a variable range of prediction errors emerged (from 0.93 to 3.32 mm according to [23]), a variable risk of bias (from low to high, according to [22,23]), and a variable size of the test set (from 5 to 574 patients according to [23]). Concerns arose on the overall estimated accuracy of the predictions, with lips and chin that emerged as the least predictable regions [22]; morphology of the predictions have been rated reasonably realistic [22].

Andlauer et al. [26] proposed a generative adversarial network strategy to enhance the accuracy of the quality of the facial texture of

post-operative simulation performed with IPS CaseDesigner® (KLS Martin Manufacturing LLC, Jacksonville, Florida, USA) [27]. A 3D stereophotogrammetry based deep learning strategy was proposed by Ter Horst et al. [28] to predict the profile of patients undergoing mandibular advancement; authors found their methodology to have a significantly higher accuracy than mass tensor model (MTM) algorithm, that is one of the most common algorithm employed in prediction software. However, only the profile was considered, losing the potentialities of a 3D representation.

Tanikawa and Yamashiro proposed a landmark-based combined with geometric morphometric method (GMM) combined with a deep neural network for regression [29]. Cross validation reported errors below 1 mm in the 54 % of the cases, reaching 100 % when the error threshold was duplicated. Ma et al. proposed a weakly supervised facial shape change prediction network (FSC–Net) and results were obtained comparable to a sota FEM method [30]. Mean errors on landmarks were comprised between 4 mm and 6 mm for both the FSC–Net and the sota method, with significant errors in the lip region. Inclusion of more patients to increase variability of cases was suggested by the authors to improve the method. Du et al. focused on mandibular segmental osteotomy [31]; a cohort of 414 patients was considered to develop a prediction model based on surface mesh theory and convolutional deep learning. Prediction errors below 2 mm were found in around 80 % in mouth region (cheilion right and left) and around 90 % on the pronasale, whilst the percentage dramatically decreased for the pogonion (53 %) and the left gonion (68 %). Differences of around 10 % emerged between right and left cheek mass (about 80 % and 88 %, respectively).

A convolutional neural network (CNN) architecture was proposed by Ali et al. [32] for diagnostic, risk stratification and post-operative face prediction. The method exploited 313 318 head CT scans. Authors reported about 93 % prediction accuracy, and prospected the reduction of operating time and costs, avoiding the long time to perform a prediction and the need for complex manual information, but a considerable number of images was needed. A considerable number of patients data were employed by Kim et al. to develop their method for the prediction of surgical movements of mandible and maxilla with graph CNN employing data from 800 patients [33]. Their work obtained interesting results, showing the potentiality of deep learning in the field when a large amount of data is available. These results and considerations are supported by the outcomes reported by Salazar et al. [21], Zhu et al. [22], Sankar et al. [23] and Almarhoumi [24] in their systematic and scoping reviews, that highlighted the necessity of further improvements in specific facial regions (particularly the lips and chin regions) to reach clinically relevant results and indicated the lack, in some case, of external validation and the use of small and uniform datasets as limitations of much current studies.

Recent literature on the topic shows that, from the most adopted mechanical modelling of human tissues to deep learning based approaches, the prediction of the behaviour of the facial soft tissues is still challenging [21–35]. In the proposed work, the prediction is realised without any type of mechanical modelling and/or mechanical characterisation of the human facial soft tissue, avoiding all the problems associated to these aspects [12]. Thus, the core of the prediction is represented by the geometrical similarity analysis, that consists in the search for facial similarities among patients affected by the same class of dental malocclusion, and by the computation of the displacement vectorial map mapping the 3D displacement of facial points from pre- to post-operative of already treated patients. Although the literature reports promising methods using artificial intelligence, in particular neural networks, the intention of this study is to keep the method as simple as possible and with a low computational cost, finding a balance between accuracy and affordability, and accessible even with limited resources. To our knowledge, the proposed approach represents a novelty in the panorama of soft tissue prediction solutions in maxillofacial field. The paper is structured as follows: in the section “Methods” the whole methodology is described; then, obtained results are reported and

discussed in the “Results” section. “Discussion and conclusions” section discusses the obtained results, strengths and limitations of the work and future developments.

The main contribution of the paper is a prediction methodology:

- based on a 3D approach without modelling of soft tissue behaviour,
- allowing, in a future development, the use of cost effective RGB-D cameras,
- requiring a short training period,
- with low computational costs.

Additionally, the methodology is designed to:

- become more robust as new patients will be added to the dataset,
- require reduced time for data preparation,
- potentially be translated into free programming languages,
- avoid the need for previously acquired specific skills.

2. Methods

A brief introduction on the construction of the 3D data employed to develop the prediction methodology is given at the beginning of this section, as a human assisted methodology previously developed and tested was adopted. The DICOM images acquired with a cone beam computed tomography (CBCT) were processed by an algorithm that performs cleaning steps to optimise the quality of the images, and the further generation of 3D depth maps. The cleaning process was aimed to remove noise from the images, and to remove the support for the head used during the acquisition; particularly, the first purpose was addressed using the Moore-Neighbor tracing algorithm [36], whilst the second purpose was addressed throughout the computation of the normalised 2D cross-correlation. Successively, the segmentation of the images was performed exploiting the spatial distribution of the coefficient of absorption for the hard tissue and the k-means algorithm for the soft tissue. A MATLAB® (MathWorks Inc., Natick, Massachusetts, USA) implementation of the marching cubes algorithm was used to construct the 3D models of the hard and soft tissue. Finally, the 3D depth maps were computed in form of square grid of points that are not connected one to another and fitting the dimension of the 3D model. This type of representation is convenient when there is no need for the entire volume acquired with the CBCT; moreover, the choice to work with this type of data allows to employ facial representation acquired with low-cost cameras [37], simplifying the acquisition process, and making it easier and faster to predict the patient’s future appearance. In fact, even if not treated in this work, the methodology could be applied directly on the depth image of a patient acquired with an RGB-D camera proved to be particularly suitable for face analysis [38,39].

2.1. Similarity analysis between patients

The fundamental hypothesis of the development of the proposed prediction methodology was that persons with a defined degree of similarity, undergoing the same type of surgery, would have a similar response to bony repositioning in terms of displacements of the soft tissue points approximating the facial surface. From this viewpoint, previous experience in face analysis for medical [6–40] and non-medical purposes [41–43] gave inspiration for this stage. To validate the methodology, only patients for whom the real post-operative was known were considered to allow a comparison between the prediction and the real outcome.

The present study followed the declaration of Helsinki protocol and was approved by the local institutional review board. Informed written consent was obtained from all the participants. Inclusion criteria were as follows: 1) maxillary hypoplasia with excess mandibular growth, 2) inadequate cheek projection, 3) class III malocclusion treated with Le Fort I (LFI) advancement and bilateral sagittal split osteotomy (BSSO)

setback, 4) completion of growth (age ranged from 21 to 43 y.o.) and 5) at least 1 year follow up. Patients with continued growth, history of craniofacial fractures or syndrome and incomplete radiological records were excluded. Patients were treated at Division of Maxillofacial Surgery, San Giovanni Battista Hospital, University of Turin. The natural head position (NHP) was adopted to position patients during CBCT scans as it provides a more physiological and realistic reference compared to conventional anatomical planes [44–46].

Seventeen patients were involved in the analysis. Due to the complexity of the repositioning of bony segments in relation to the small sample available, limited inclusion criteria for surgery type have been necessary. Previous studies in the literature have mainly focused on a limited set of surgical movements [18–33].

For the development of the methodology, patients underwent Le Fort I (LFI) advancement and bilateral sagittal split osteotomy (BSSO) setback (class III malocclusion) were considered. To perform the similarity analysis among patients considering the malocclusion class, an approach based on facial proportions computed on soft tissue interlandmarks distances was adopted. The list of the cephalometric landmarks used is reported in Table 1; definitions relied on Swennen’s cephalometric atlas [47]. Eleven proportions were defined from these distances partially basing on the work by Ulrich et al. [48]. Table 2 reports the proportions involved and defines the distances between which they are computed.

The differences between the corresponding proportions of the test patient, i.e., the patient whose post-operative is to be predicted, and of the patients in the similarity group were calculated (pairwise comparison); the results of the differences were added up and the lowest result indicated which patient was the most similar to the test patient. In Fig. 1, the similarity analysis is schematised.

2.2. Displacement vectorial map

The displacement vectors of the facial points from the most similar patient were used to generate the prediction. This section details the computation of the displacement vectorial map. To ensure accuracy, only patients with complete pre- and post-operative CBCT scans of acceptable quality were considered (Fig. 2 and Fig. 3).

To focus the analysis on the facial regions most affected by surgery, a region of interest (ROI) was defined. Specifically, a spherical ROI was created, centered at the pronasale, with a radius corresponding to the distance between the pronasale and the right zygion. This approach allowed excluding areas of the face less impacted by surgical movements. Fig. 4 illustrates an example of the selected subset of soft tissue points. The same procedure was applied to both the pre- and post-operative depth maps.

Table 1

List of the cephalometric landmarks used according to Swennen’s definitions.

Landmark’s name	Landmark’s definition
Nasion	Midpoint of the soft tissue contour of the base of the nasal root at the level of the frontonasal suture.
Exocanthion	Soft tissue point located at the outer commissure of each eye fissure.
Endocanthion	Soft tissue point located at the inner commissure of each eye fissure.
Pronasale	The most anterior midpoint of the nasal tip.
Subnasale	The point at each margin of the midportion of the columella crest.
Alare	The most lateral point on each alar contour.
Labiale superius	The midpoint of the vermillion line of the upper lip.
Cheilion	The point located at each labial commissure.
Gonion	The most lateral point on the soft tissue contour of each mandibular angle.
Sublabiale	The most posterior midpoint on the labiomental soft tissue contour that defines the border between the lower lip and the chin.

Table 2
List of the proportions considered for the similarity analysis.

Proportions	
$\frac{ex_l-ex_r}{n_prn + prn_sl}$	<ul style="list-style-type: none"> • ex_l-ex_r: distance between left and right exocanthion; • n_prn: distance between nasion and pronasale; • prn_sl: distance between pronasale and sublabiale.
$\frac{ex_l-ex_r}{en_l-en_r}$	<ul style="list-style-type: none"> • en_l-en_r: distance between left and right endocanthion.
$\frac{ex_l-ex_r}{n_prn + prn_sl}$	
$\frac{en_l-en_r}{n_prn}$	
$\frac{ex_l-ex_r}{prn_sl}$	
$\frac{n_prn}{n_sn}$	<ul style="list-style-type: none"> • n_sn: distance between nasion and subnasale;
$\frac{n_prn}{n_sl}$	<ul style="list-style-type: none"> • n_sl: distance between nasion and sublabiale.
$\frac{prn_sl}{n_sl}$	<ul style="list-style-type: none"> • sn_sl: distance between subnasale and sublabiale.
$\frac{n_sl}{en_l-en_r}$	
$\frac{n_sn}{en_l-en_r}$	<ul style="list-style-type: none"> • n_ls: distance between nasion and labiale superius.
$\frac{n_ls}{ala_l-ala_r}$	<ul style="list-style-type: none"> • ala_l-ala_r: distance between left and right alare.
$\frac{ala_l-ala_r}{n_sn}$	

2.2.1. Pre- and post-operative depth maps alignment

To quantify the displacement of facial surface points, the pre- and post-operative depth maps needed to be aligned within the same reference system. For this purpose, a human-assisted approach was employed, incorporating the Iterative Closest Point (ICP) algorithm [49, 50]. This alignment step was crucial, as any inaccuracy could lead to an unreliable displacement vectorial map, ultimately compromising the predictive accuracy of the methodology.

Aligning soft tissue depth maps presents a non-trivial challenge due to variations in facial and head poses, as well as the surgical modifications undergone by patients. To address this, a stable reference area on the hard tissue, uninvolved in any corrective surgeries, was selected for computing the transformation matrix (Fig. 5). The extracted hard tissue sub-regions were then denoised and down-sampled before being processed by the ICP algorithm. To enhance registration accuracy, an initial coarse estimation of the rigid transformation was computed based on the centroids of the two point clouds.

Alignment accuracy was assessed using the root mean square error (RMSE) of the final ICP iteration, with a threshold set at 2 mm, corresponding to half of the maximum acceptable error in landmark localization [51–54]. Once the optimal rigid transformation was computed, it was applied to the entire post-operative hard and soft tissue point clouds. The transformed coordinates were then used to reconstruct the new 3D depth maps (Fig. 6 and Fig. 7).

Qualitative analysis (Fig. 8) reveals that in the post-operative point cloud (red), mandibular points are retracted relative to their pre-operative counterparts (green), while maxillary points are advanced. This displacement pattern aligns with the clinical context, as the patients

were affected by prognathism and underwent BSSO setback and LF I advancement.

2.2.2. Pre-to-post operative vectorial map

After the registration step, the Euclidean distances were computed between corresponding points on pre- and post-operative; only the points of the spherical subset were considered. To enhance the accuracy of the computation, the two facial subsets were equalised in order to have the same number of points. A vectorial map of the displacement of each point was constructed, considering the X, Y, Z components separately. This way, the information about the modulus and the versor of the displacement vector of each point was preserved. Fig. 9 represents the displacement vectorial map of one of the considered patients.

2.3. Generation of the predicted facial depth map

To generate the predicted depth map, the displacement vectorial map of the most similar patient was applied to the pre-operative of the test patient. During the development of the methodology, the possibility of involving the soft tissue thickness (STT) of specific landmarks as a feature to forecast the facial surface was considered; in fact, potential changes in the soft tissue thickness after orthognathic surgeries could give crucial information in the construction of the predicted face. Notwithstanding, a previous study showed that any significant modification occurred in the values of the STT of orthognathic patients after the interventions [55], thus this information was dismissed. In Fig. 10, the prediction for one of the test patients is shown. Euclidean distances between predicted and real facial points positions were computed to quantify the prediction error for each soft tissue point; Wilcoxon signed-rank test was computed on the predicted and real landmarks to evaluate the statistical significance of discrepancies in X,Y,Z dimensions.

To make the prediction closer to a real visualisation, a 3D model was generated from the 3D depth map, and it was texturized using an RGB image of the test patient. This stage was developed in Blender® (Blender Foundation). The texturing of the 3D model was performed throughout the UV mapping problem, that allows to wrap a 2D texture map around a 3D object.

3. Results

To explore the effectiveness of the proposed methodology, a prediction of the aspect of the face was realised for two patients who received maxillofacial surgeries. This way, a comparison with the real post-operative was possible and consequently a quantification of the prediction error. Due to the inclusion criteria set for the study, the methodology was tested only for LFI advancement osteotomy and BSSO setback. Fig. 11 and Fig. 12 illustrate the superimposition of the predicted and real facial surfaces, visualised as 3D meshes, for both test patients.

Prediction errors were computed as Euclidean difference between

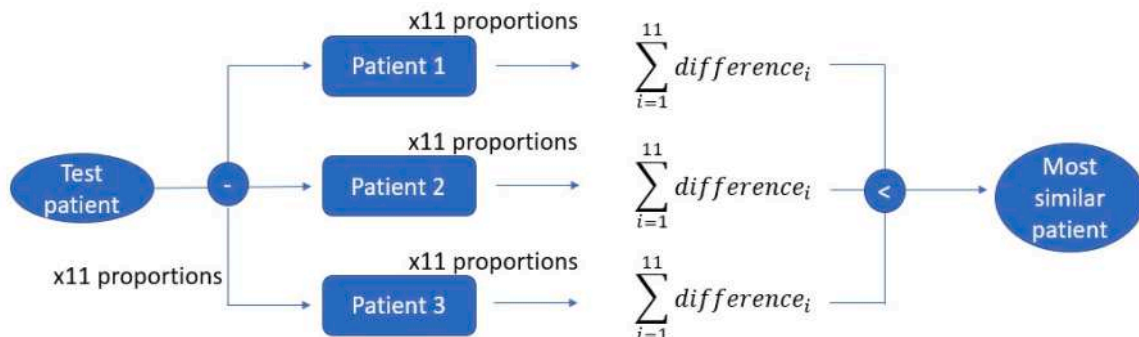


Fig. 1. Schematic representation of the proposed methodology to assess the similarity among subjects with the same malocclusion.

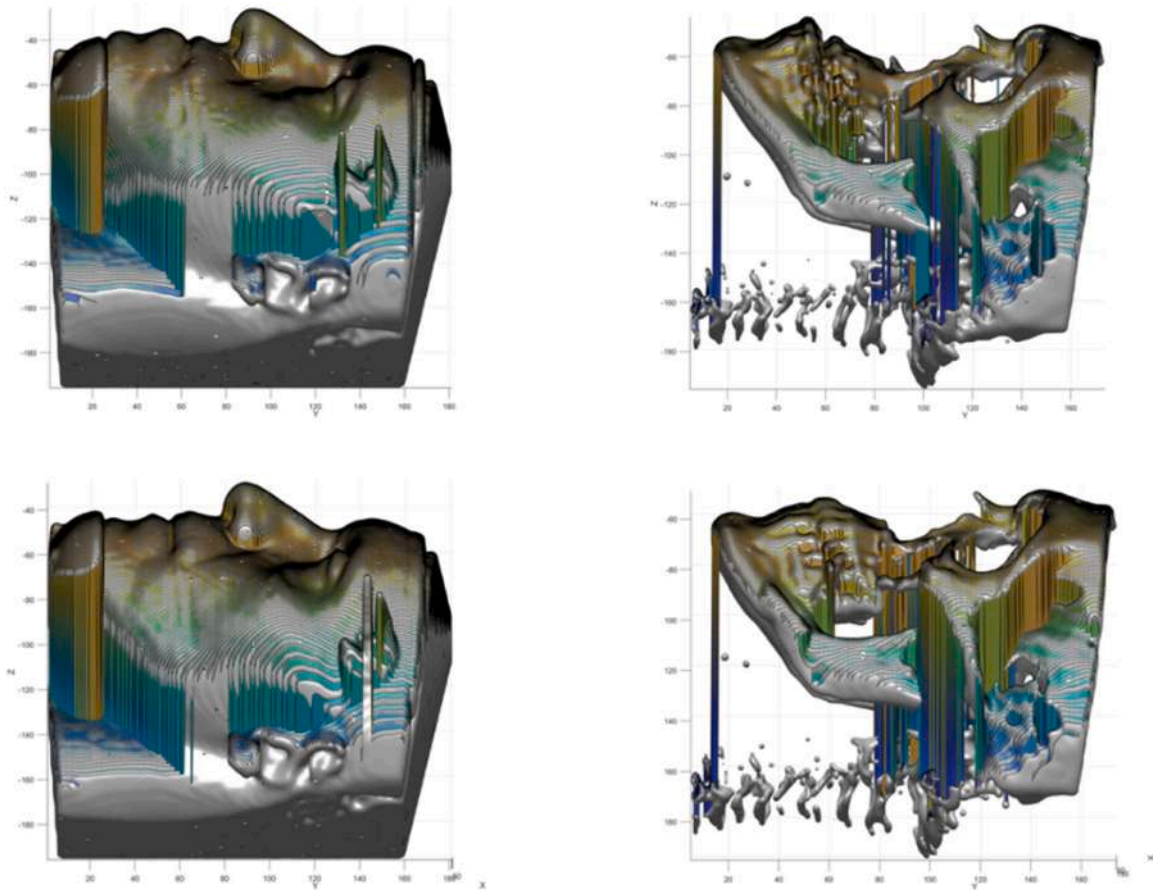


Fig. 2. Pre- (above) and post-operative (below) of one of the test patients. Superimposition of the 3D models and depth maps is reported. Measures are reported in mm.

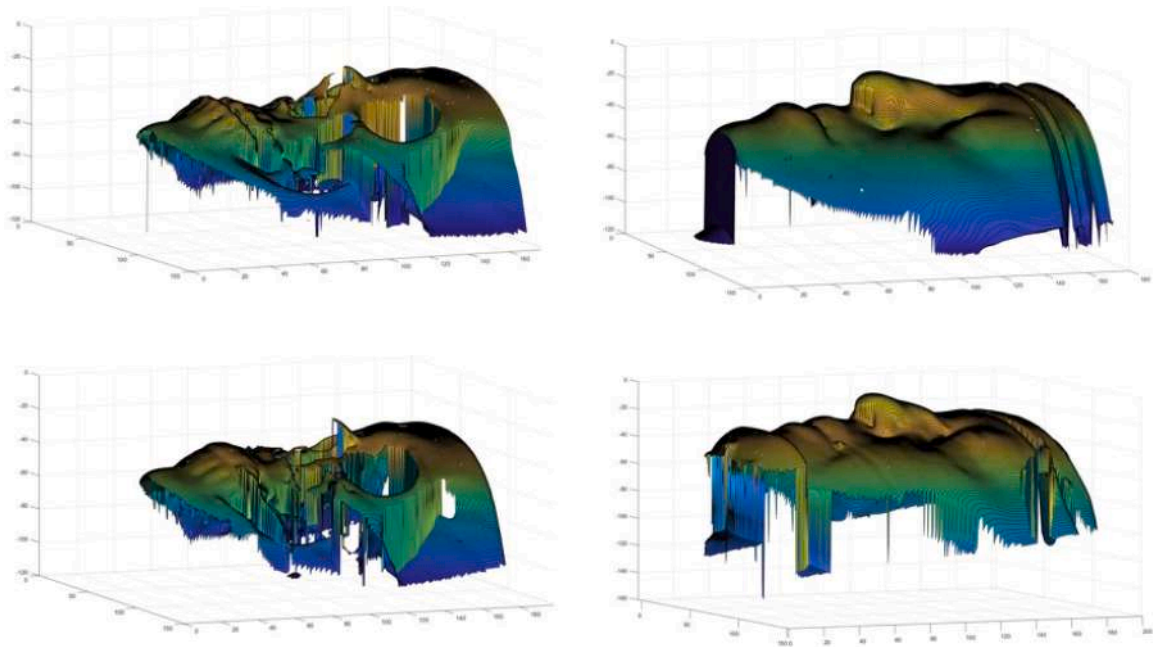


Fig. 3. Pre-(above) and post-(below) operative 3D depth maps of one of the considered patients. Measures are reported in mm.

the surface points of the predicted map and the real post operative map. A subset of points corresponding to the previously defined spherical subset was selected for both prediction and real facial map. Thus, an

error map highlighting different error ranges was obtained. Fig. 13 shows the superimposition of the real post-operative and the prediction for one of the two patients used as test. Considering that the proposed

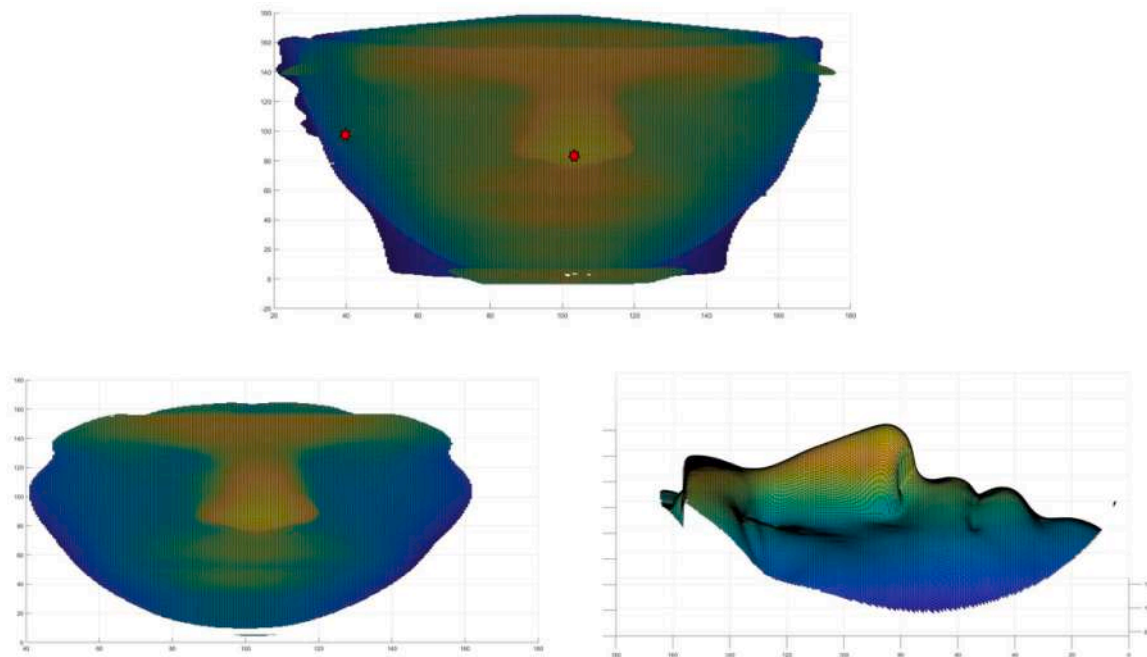


Fig. 4. Above: complete 3D facial depth map with the pronasale and right zygion landmarks highlighted (red points). Below: spherical subset of the facial points, frontal (left) and lateral (right). Measures are reported in mm.

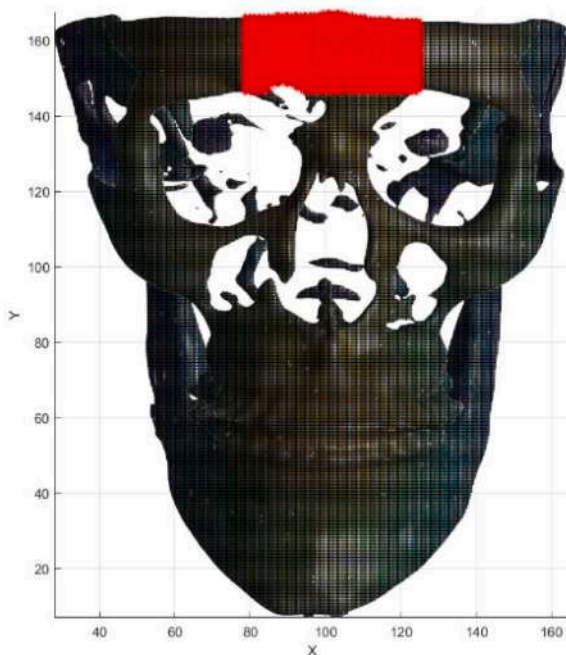


Fig. 5. Fixed hard tissue area (red) considered for the computation of the rigid transformation. Measures are reported in mm.

methodology is landmark-based, it could be reasonable to set the acceptable error to 4 mm as it is reported in previous literature as the maximum acceptable error in landmark positioning [51–54]; taking into account previous studies [12–33], the acceptable error threshold was set to 2.5 mm. Fig. 14 depicts the error map for the first test patient with different colours according to different error ranges: red for points with errors greater than 9 mm, yellow for errors in the range 4–9 mm, blue for errors between 3 mm and 4 mm, black for errors between 2.5 mm and 3 mm and green for errors below 2.5 mm. To provide a more detailed

analysis of the results, errors below 4 mm were categorised into smaller ranges. Considering the total number of predicted points, the majority of errors was below 2.5 mm (71.25 %), 9.93 % of points were in the range 2.5–3 mm, 10.61 % were in the range 3–4 mm, 7.50 % were in the range 4–9 mm and 0.72 % were greater than 9 mm.

Fig. 15 depicts the error map for the second test patient. The majority of errors was below the acceptable error threshold (69.9 %), whilst 10.25 % of the total points was between 2.5 mm and 3 mm, 9.60 % was between 3 mm and 4 mm, 9.37 % was between 4 mm and 9 mm and 0.84 % was greater than 9 mm.

For both predictions, most points fell below the acceptable threshold. The highest errors were concentrated along the outline, particularly around the left gonion and the outer area near the exocanthion. The maximum error was found around the left gonion in both tests, with a lower concentration of errors around the left and right alares.

The Wilcoxon signed-rank test was applied to test the differences between the position of the landmarks on the predicted and the real maps, with a 95 % confidence level. Predicted landmarks represented the first data group, the post-operative landmarks the second data group. Each dimension (X,Y,Z) was tested separately, to investigate the source of the errors. For the first test patient, statistically significant differences were observed for the gonion and cheilion in the Z direction ($p = 0.03$), whereas no statistical significance was found for the other landmarks in all dimensions. P-values greater than 0.05 were obtained for the remaining landmarks in all dimensions. For the second test patient, p-values exceeded 0.05 for all landmarks in the X, Y, and Z dimensions, except for the gonion in Z dimension, indicating that the positional differences were not statistically significant for the majority of the involved cephalometric points.

4. Discussion and conclusions

The proposed study explored the suitability of a simple, computationally low expensive solution for the prediction of the displacement of facial points after orthognathic surgeries. Several considerations can be drawn basing on the obtained results; in fact, errors in the eyes regions were predictable due to two main issues: 1) the configuration (open/close) of the eyes during the acquisition, which was not the same for all

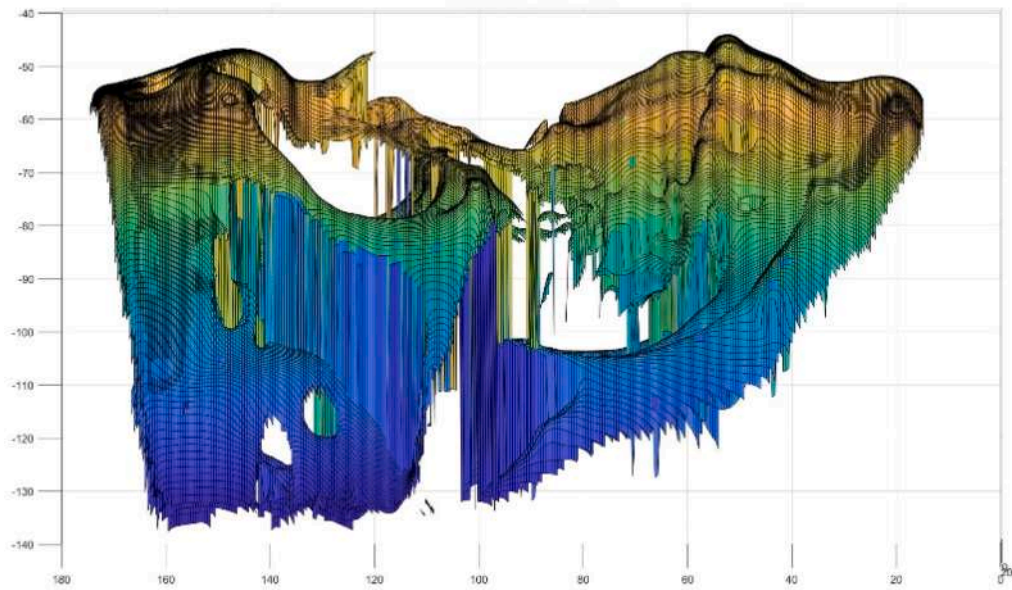


Fig. 6. Registered pre- and post-operative hard tissue. Measures are reported in mm.

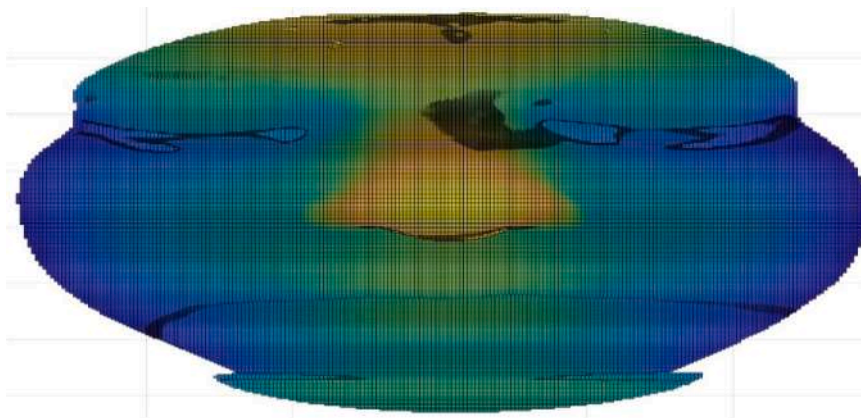


Fig. 7. Registered pre- and post-operative soft tissue (frontal view). Measures are reported in mm.

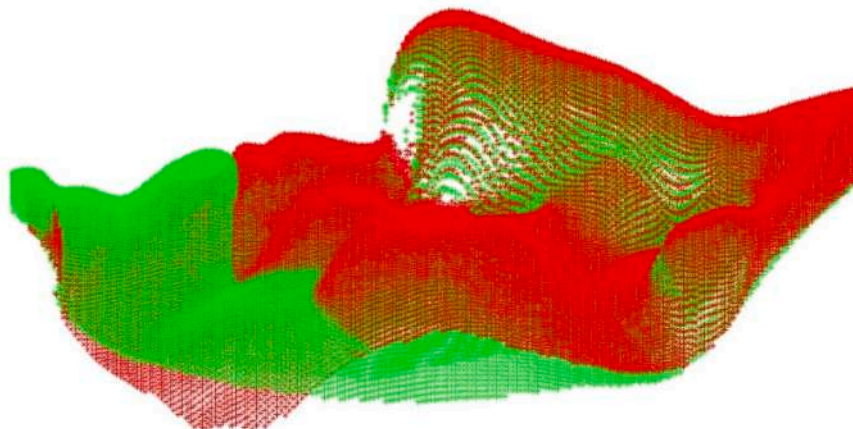


Fig. 8. Soft tissue pre- (green) and post- (red) operative after the application of the rigid transformation. Point cloud visualisation (lateral view).

patients and was not the same in some cases for the same patient in the pre- and in the post-operative, and 2) the inter-personal variability associated with the eye size. The latter issue was partially addressed

with the landmark-based similarity analysis, in which the proportion between left and right exocanthion distance and left and right endocanthion distance was considered, among the others, to determine the

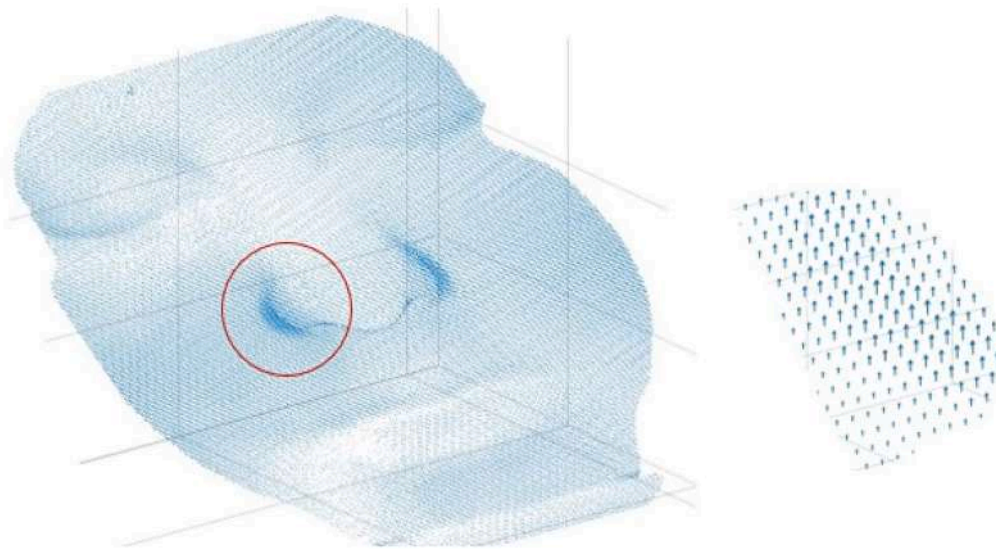


Fig. 9. Displacement vectorial map mapping the movements of each point from the pre- to the post-operative of a patient underwent LF I osteotomy advancement and BSSO setback. On the right, a detailed view is reported.

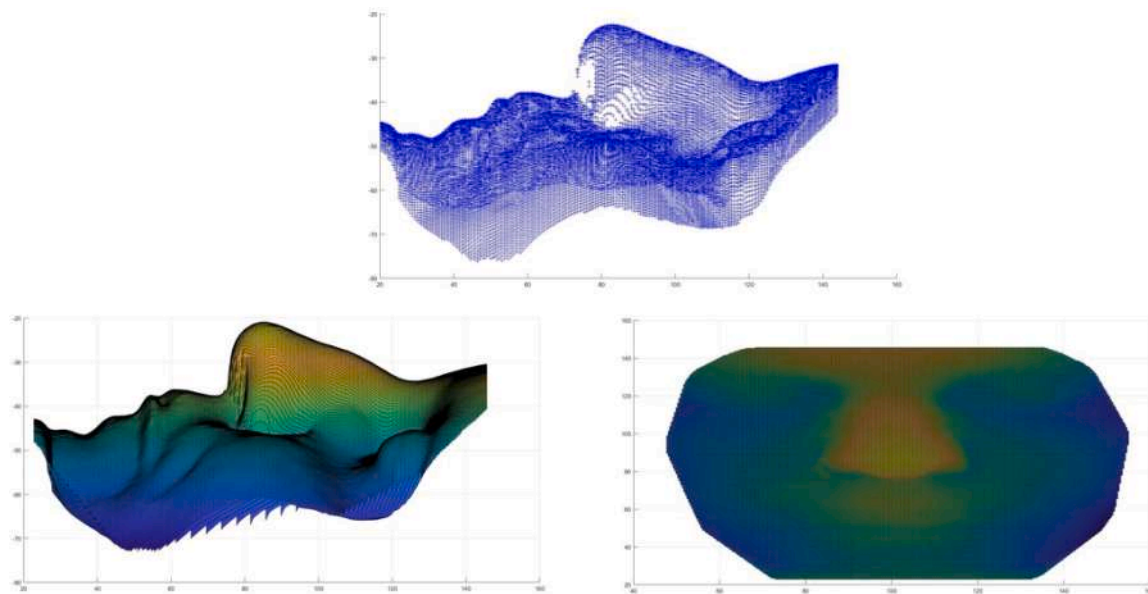


Fig. 10. Prediction of the facial aspect of one of the two test patients. The figure depicts the prediction in form of point cloud (above), the lateral (below, left) and the frontal (below, right) views of the 3D depth map. Measures are expressed in mm.

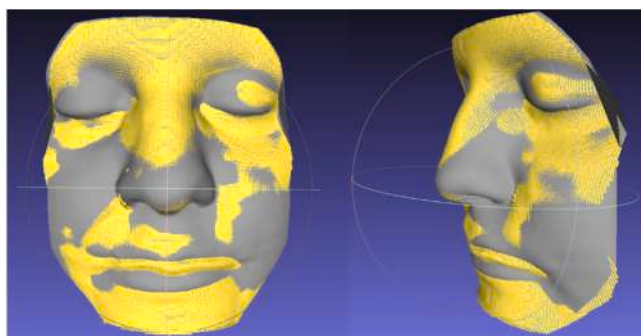


Fig. 11. Real (gray) and predicted (yellow) surface 3D mesh of the first test patient.

most similar patient; moreover, these measurements were involved in seven out eleven proportions. Quite the opposite, the former issue was not fixable. Even if further variability was introduced, the inconsistencies in eyes states offered the opportunity to test the feasibility of the proposed methodology in a “worst case” scenario. Future studies will address the problem integrating the data acquisition protocol with indications on maintaining a same neutral face expression in all scans.

Concerning the errors detected around the left and right alare, a similar consideration can be made on the inter-personal variability of the size of the nose, which was only partially addressed in the landmark-based similarity analysis with the evaluation of the inter-alares distance. Moreover, in the case of the nose width, the evaluation was also affected by the optional suture of the alar wings (alar cinch) performed to prevent an excessive increasing of the alar width. The need for the alar cinch suture and its extent are typically assessed by the surgeon during

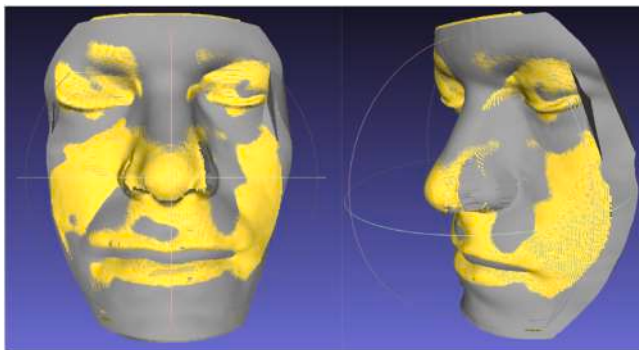


Fig. 12. Real (gray) and predicted (yellow) surface 3D mesh of the second test patient.

surgery rather than in the preoperative planning. As a result, this factor could influence the prediction of the alar points' positions. However, since no data were available to account for it, it was not considered in the computation of the displacement vectorial map. A different consideration should be made to analyse the distribution of the errors on the left side of the map (left gonion region); particularly, during the development of the alignment process, a slight tendency towards misalignment in the x direction was found. To evaluate the quality of the alignment, the RMSE computed on the last ICP iteration was considered; a RMSE <2 mm was judged to be an indicator of sufficient accuracy, as it was half of the maximum acceptable error for landmark positioning indicated in previous studies [51–54], and it is considered clinically acceptable. Even if the registration met this requirement, inaccuracies could have been introduced in the computation of the Euclidean distances, and consequently in the prediction, but resulting in acceptable error values for most of the points. On the other hand, it is to be noticed that, in previous literature, a mismatch between prediction accuracy for left and right side is documented [31]. In this work, the issue of a slight misalignment could be due to the fact that, for the registration process, only the coordinates of the depth map were considered, i.e., only a portion of the entire volume. Despite a possible overcoming of this aspect could be obtained by laterally extending the region of the forehead considered to compute the registration matrix, in this work it was chosen to use only a frontal portion to develop a method that could be applied to facial data obtained with different technologies, in particular

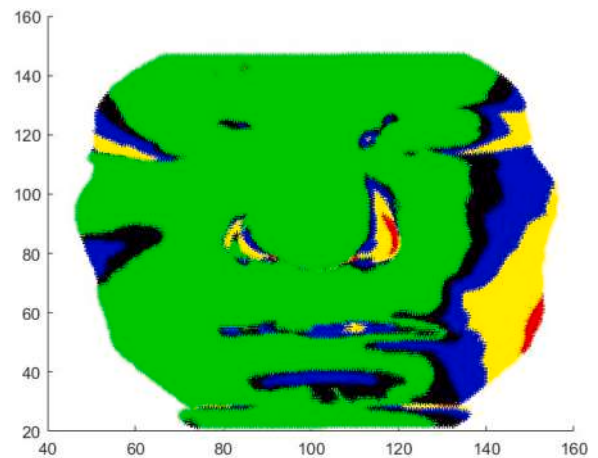


Fig. 14. Error map for the first test patient computed as Euclidean distance between corresponding points of the post-operative and the prediction. Red points correspond to errors greater than 9 mm; yellow points correspond to errors between 4 mm and 9 mm, blue points correspond to errors between 3 mm and 4 mm, black points correspond to errors between 2.5 mm and 3 mm and green points correspond to errors <2.5 mm.

RGB-D cameras. This type of acquisition technology usually requires frontal scans. The involvement of a larger portion or the entire 3D model could be considered to improve the computation of the rigid transformation, but further development of the methodology would be necessary to integrate the two types of acquisition technology. Future development of this research will be aimed at addressing this aspect.

Qualitative considerations can be made on Fig. 16 and Fig. 17, depicting respectively the upper and the lower face of the first test patient. The lateral view reported in Fig. 16 shows how the predicted points, depicted in red, define a shape that is highly consistent with the real one, depicted in blue. Considering that the forehead and the superior nasal region were not affected by surgical procedures, and consequently, should have the same shape in the pre- and in the post-operative (real and predicted), this consistency suggests the robustness of the registration process (also suggested by Fig. 6) despite the slight misalignment in x direction and of the whole prediction methodology. The qualitative assessment was conducted by two expert maxillofacial surgeons, who rated the predicted 3D facial surfaces as acceptable.

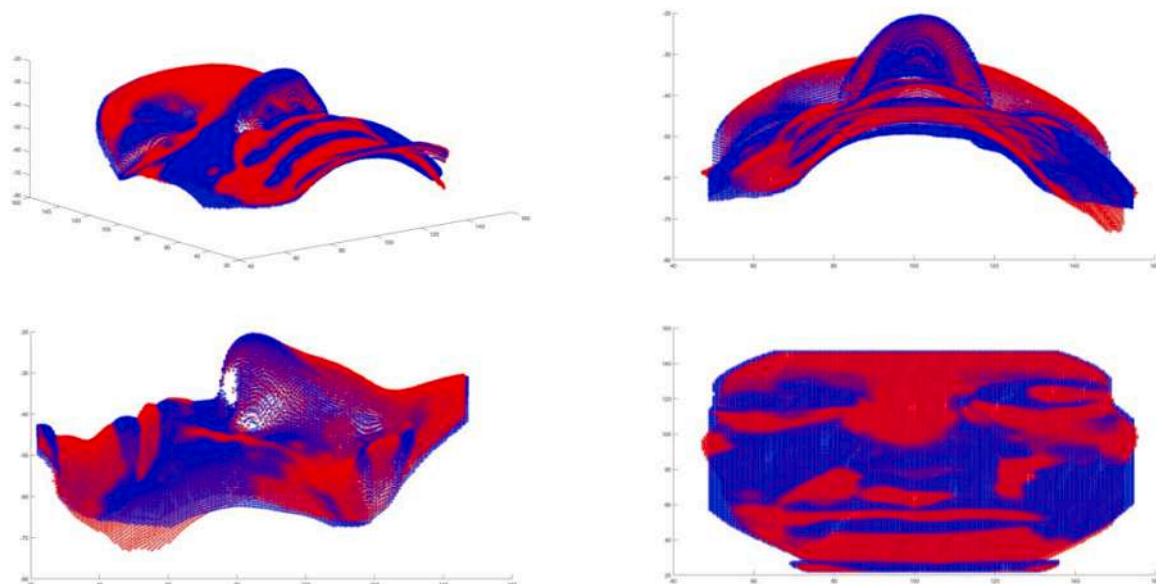


Fig. 13. Superimposition of the real post-operative (blue) and the predicted (red) point clouds for the first test patient. Measures are reported in mm.

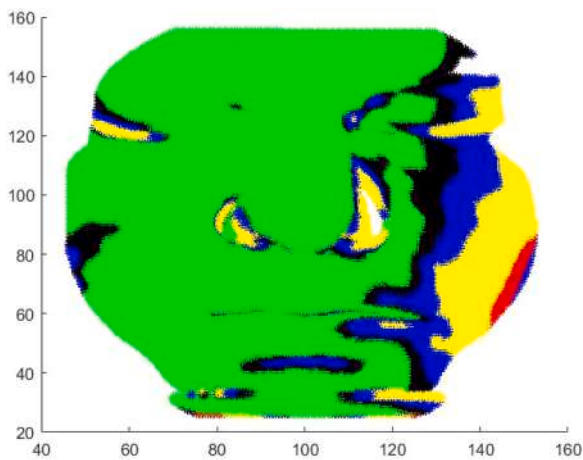


Fig. 15. Error map for the second test patient computed as Euclidean distance between corresponding points of the post-operative and the prediction. Red points correspond to errors greater than 9 mm; yellow points correspond to errors between 4 mm and 9 mm, blue points correspond to errors between 3 mm and 4 mm, black points correspond to errors between 2.5 mm and 3 mm and green points correspond to errors less than 2.5 mm.

In the evaluation of commercial solutions for predicting soft tissue appearance, the lips have been identified as particularly prone to errors [12]. This issue has also been reported in approaches beyond mechanical modelling, underscoring the challenges in accurately predicting the displacement of these regions [21–31]. In Fig. 17 it is visible that the predicted shape (red) is consistent with the shape of the real post-operative (blue) for the upper lip, and it presents a slight underestimation of the z coordinates for the lower lip. As reported for the eyes, a slight difference in the configuration of the mouth (open/close) could lead to an inaccurate computation and/or application of the displacement vectorial map. Consequently, it resulted in the application of the pre-to-post-operative vectors also to points located between upper and lower lips, but with errors below or slightly above the acceptable threshold. This could be due to the fact that even a small change in facial expression, particularly of the mouth, can result in considerably different displacements of the lips, in addition to the fact that lips do not rely on bony structures. Lastly, the prediction shows a slight overestimation of the z coordinate of points comprised between the lower lip and the chin; this area, and therefore the displacement vectorial map, is affected by the presence of the chin support. However, the error map showed that the majority of the points were under the error threshold, and the shape of the predicted surface is consistent with the

post-operative one. This can be ascribed to the fact that the chin support was used during the acquisition of the most similar patient as well as the acquisition of the post-operative of the test patient, leading to a similar deformation of the soft tissue. Similar considerations can be made for the second test patient.

The quantitative analysis of the errors conducted on both the complete prevision (coordinates of all the facial points) and on the landmarks (coordinates of the cephalometric landmarks) highlighted that, despite the limited number of patients included in the study, results consistent with previous studies were obtained. Concerning the assessment of the complete prevision, the error maps highlighted that for the two test patients, most of the errors were < 2.5 mm, considered acceptable in previous literature [12–33], where errors on single landmarks of around 4 mm [30] or more [56] were reported. In this viewpoint, about 70 % of the total number of predicted positions differed from the real positions by < 2.5 mm, and around 90 % by < 4 mm. These considerations become even more relevant in light of the qualitative analysis, which highlighted the consistency between the predicted and the real facial shape.

The Wilcoxon signed-rank test performed on the landmarks coordinates of the two test predictions confirmed the potentiality of the proposed methodology; statistically significant differences ($p < 0.05$) between the positions of the predicted and the real landmarks emerged only for gonion and cheilion (first test patient) and cheilion (second test patient), out of a total of 15 landmarks considered. The number of landmarks tested is higher than in a number of previous studies, which tested reduced sets of landmarks and/or relied mainly on a single plane [12–33].

The present study is subject to certain limitations, the primary one being the size of the database due to the adopted inclusion criteria for patients from a single centre. Several factors should be considered as the proposed method is designed to become more robust as the number of patients in the similarity analysis database increases. The dataset should include an adequate representation of the variability of the facial proportions of patients with dysmorphism. The data coverage allows to compute the optimal size taking into account the level of confidence, the variance of the input features and the desired precision. In case of the 95 % level of confidence and a desired precision of 0.05, considering the variance of the features in the actual database, a size of around 1160 subjects would be required. A second issue could be related to the curse of dimensionality. In the case of the proposed method, the number of features has been selected to find a balance between dataset size and number of features. With the increase of the dataset size, learning curves will be considered and potentially techniques of feature selection or feature extraction and dimensionality reduction (e.g., a reduction of the number of considered landmarks) will be adopted. This required size is

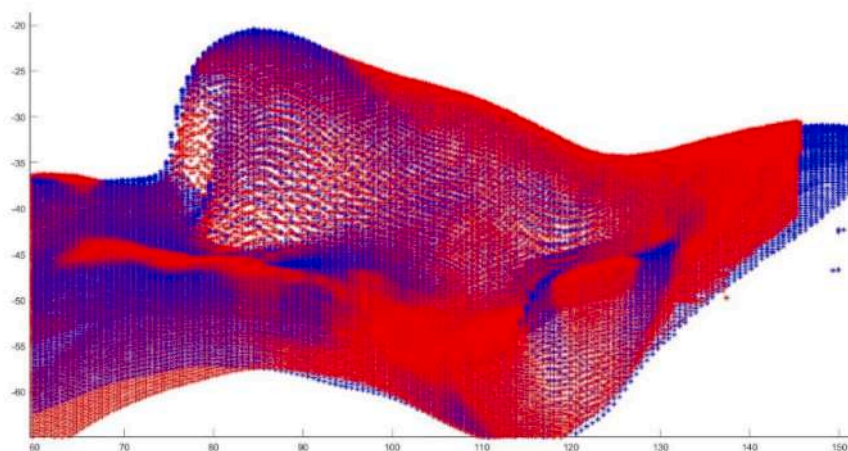


Fig. 16. Superimposition of the real post-operative (blue) and the predicted points (red) in form of point clouds (detail of the superior half of the face).

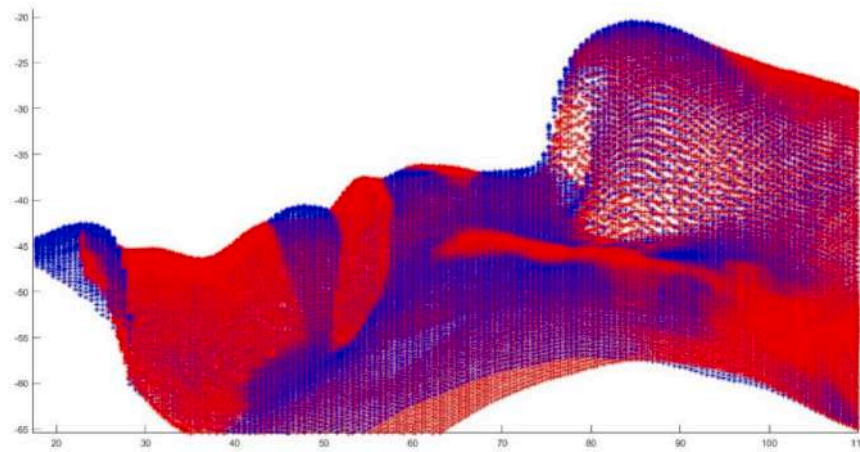


Fig. 17. Superimposition of the real post-operative (blue) and the predicted points (red) in form of point clouds (detail of the inferior half of the face).

substantially lower than that reported in previously presented studies [32,33], where deep learning-based approaches were adopted, and errors were obtained comparable to those of the present study. However, future studies will be conducted on different types of surgeries to test the universality of the proposed approach and its limitations.

The development of a simple method aims to provide a tool that is easily usable and understandable by users with diverse backgrounds, while ensuring acceptable levels of accuracy. Moreover, the choice to avoid deep learning techniques allows for the implementation of low computational cost solutions, offering several advantages. A method with these characteristics is more accessible, as it can be executed on tablets or PCs without requiring high-performance GPUs. Furthermore, the algorithm's lightweight nature facilitates its implementation even in resource-limited settings.

The results obtained in this exploratory study, although on a small sample, suggest that the method can effectively balance accuracy and accessibility. Indeed, further experimentations are needed, but the proposed method showed the potentialities of a simple, traditional approach. An example of the potentialities of simple solutions in the field of facial prediction is represented by the work of Suh et al. [56], in which the sparse partial least squares regression method has achieved acceptable results. In their study, 2D data from 318 patients were analyzed, from which 34 input variables were extracted. Contrarily, in this study, 3D data were used, and a reduced number of input variables was considered.

Lastly, some consideration can be made on the potential reduction of costs. In fact, the type of data employed, i.e., 3D depth maps, could lead to a reduction of the costs as it can be acquired with cost-effective cameras apt to facial analysis applications. An additional reduction of the costs is represented by the fact that the entire methodology, also referring to the human assisted processing of data, is implemented in the MATLAB environment but can be translated in a free programming language such as Python. No special training is required for the use of the proposed solution except for the correct positioning of the landmarks, which considerably reduces the time needed to acquire specific skills and reduces time for data preparation. Furthermore, the human assisted methodology for data processing reduces the time for data preparation. The overall conclusion can be drawn that the proposed methodology, considering the limitations of the study, produced a good approximation of the real post-operative of the tested patients while maintaining user-friendliness with low computational resources.

Ethical approval

This study was performed in line with the principles of the Declaration of Helsinki. Approval was granted by the local institutional

review board (No. 574.037). Informed consent was obtained from all individual participants included in the study.

Consent for publication

Patients signed informed consent regarding publishing their data and photographs.

CRediT authorship contribution statement

Elena Carlotta Olivetti: Writing – original draft, Visualization, Software, Methodology, Investigation, Formal analysis, Data curation, Conceptualization. **Federica Marcolin:** Writing – review & editing, Supervision, Methodology, Conceptualization. **Sandro Moos:** Writing – review & editing, Visualization, Supervision, Software, Methodology, Data curation. **Enrico Vezzetti:** Writing – review & editing, Supervision, Resources, Project administration, Funding acquisition. **Claudia Borbon:** Writing – review & editing, Validation, Investigation, Conceptualization. **Emanuele Zavattero:** Writing – review & editing, Validation, Supervision, Investigation, Conceptualization. **Guglielmo Ramieri:** Writing – review & editing, Supervision, Resources, Project administration, Funding acquisition.

Declaration of competing interest

The authors declare the following financial interests/personal relationships which may be considered as potential competing interests: Elena Carlotta Olivetti has patent pending to Politecnico di Torino (assignee). Federica Marcolin has patent pending to Politecnico di Torino (assignee). Sandro Moos has patent pending to Politecnico di Torino (assignee). Enrico Vezzetti has patent pending to Politecnico di Torino (assignee). Claudia Borbon has patent pending to Politecnico di Torino (assignee). Emanuele Zavattero has patent pending to Politecnico di Torino (assignee). Guglielmo Ramieri has patent pending to Politecnico di Torino (assignee). If there are other authors, they declare that they have no known competing financial interests or personal relationships that could have appeared to influence the work reported in this paper.

Acknowledgements

The authors would like to thank the project “3D-Surgeered - Pre-surgery planning by means of 3D modelling” of Department of Management and Production Engineering of Politecnico di Torino.

Funding sources

This research did not receive any specific grant from funding agencies in the public, commercial, or not-for-profit sectors.

References

- [1] A. Cuccia, C. Caradonna, «The relationship between the stomatognathic system and body posture», *Clinics* 64 (2009) 61–66, <https://doi.org/10.1590/S1807-59322009000100011>, gen.
- [2] A. Marchena-Rodríguez, N. Moreno-Morales, E. Ramírez-Parga, M.T. Labajo-Manzanares, A. Luque-Suárez, G. Gijón-Noguero, «Relationship between foot posture and dental malocclusions in children aged 6 to 9 years», *Medicine* 97 (19) (2018) <https://doi.org/10.1097/MD.00000000000010701> fascp. e0701, mag.
- [3] G. Perinetti, L. Contardo, A. Silvestrini-Biavati, L. Perdoni, e A. Castaldo, «Dental malocclusion and body posture in young subjects: a multiple regression study», *Clinics* 65 (2010) 689–695, <https://doi.org/10.1590/S1807-59322010000700007>.
- [4] A.J. Pérez-Belloso, M. Coheña-Jiménez, M.E. Cabrera-Domínguez, A.F. Galan-González, A. Domínguez-Reyes, e M. Pabón-Carrasco, «Influence of dental malocclusion on body posture and foot posture in children: a cross-sectional study», *Healthcare* 8 (4) (2020) <https://doi.org/10.3390/healthcare8040485> fascArt. fasc. 4, dic.
- [5] B. Isaila, et al., «Analysis of dental malocclusion and neuromotor control in young healthy subjects through new evaluation tools», *J. Funct. Morphol. Kinesiol.* 4 (2019) <https://doi.org/10.3390/jfkm4010005> fasc. 1, Art. fasc. 1, mar.
- [6] G. Gerbino, et al., «Malar augmentation with zygomatic osteotomy in orthognathic surgery: bone and soft tissue changes three-dimensional evaluation», *J. Cranio-Maxillofac. Surg.* (2021) <https://doi.org/10.1016/j.jcms.2021.01.008> gen.
- [7] M.Y. Mommaerts, *The surgical art of facial makeover: planning and operative techniques. A comprehensive guide to orthofacial surgery*, Orthoface R & D GCV (2013).
- [8] W.C. Shaw, M. Addy, e C. Ray, «Dental and social effects of malocclusion and effectiveness of orthodontic treatment: a review», *Commun. Dent. Oral Epidemiol.* 8 (1) (1980) 36–45, <https://doi.org/10.1111/j.1600-0528.1980.tb01252.x>, fasc.
- [9] E. Atik, M.M. Önde, S. Donnori, S. Tutar, e O.C. Yiğit, «A comparison of self-esteem and social appearance anxiety levels of individuals with different types of malocclusions», *Acta Odontol. Scand.* 79 (2) (2021) 89–95, <https://doi.org/10.1080/00016357.2020.1788720>, fascFeb.
- [10] D. Claudino, e J. Traebert, «Malocclusion, dental aesthetic self-perception and quality of life in a 18 to 21 year-old population: a cross section study», *BMC Oral Health* 13 (2013) 3, <https://doi.org/10.1186/1472-6831-13-3>, volfasc. 1gen.
- [11] W.R. Proffit, R.P. White, e D.M. Sarver, *Contemporary Treatment of Dentofacial Deformity*, Mosby St, Louis, 2003 vol. 283.
- [12] E.C. Olivetti, et al., «3D Soft-tissue prediction methodologies for orthognathic surgery—A literature review», *Appl. Sci.* 9 (2019) 4550, <https://doi.org/10.3390/app9214550>, fasc. 21gen.
- [13] P.S. Fleming, «Orthodontic treatment planning: can we plan for stability?», *Br. Dent. J.* 230 (2021) <https://doi.org/10.1038/s41415-021-2891-5> volfasc. 11, Art. fasc. 11, giu.
- [14] M. Hertanto, A.F. Ayoub, P.C.M. Benington, K.B. Naudi, e P.S. McKenzie, «Orthognathic patient perception of 3D facial soft tissue prediction planning», *J. Cranio-Maxillofac. Surg.* (2021) <https://doi.org/10.1016/j.jcms.2021.03.009> apr.
- [15] N. Bergkulla, et al., «Introduction and assessment of orthognathic information clinics», *Eur. J. Orthod.* 39 (6) (2017) 660–664, <https://doi.org/10.1093/ejo/cjx025>, volfascnov.
- [16] Y.-J. Chang, A.C.O. Ruellas, M.S. Yatabe, P.M. Westgate, L.H.S. Cevidanes, e S. N. Huja, «Soft tissue changes measured with three-dimensional software provides new insights for surgical predictions», *J. Oral Maxillofac. Surg. Off. J. Am. Assoc. Oral Maxillofac. Surg.* 75 (10) (2017) 2191–2201, <https://doi.org/10.1016/j.joms.2017.05.010>, volfascott.
- [17] A. Modabber, et al., «Comparison of soft tissue simulations between two planning software programs for orthognathic surgery», *Sci. Rep.* 12 (2022) 5013, <https://doi.org/10.1038/s41598-022-08991-7>, fasc. 1, pmar.
- [18] K.J.C. Lee, S.L. Tan, H.Y.A. Low, L.J. Chen, C.W. Yong, e M.T. Chew, «Accuracy of 3-dimensional soft tissue prediction for orthognathic surgery in a Chinese population», *J. Stomatol. Oral Maxillofac. Surg.* (2021) <https://doi.org/10.1016/j.jormas.2021.08.001> ago.
- [19] M.R. Philip, e R. AlFotawi, «The accuracy of soft tissue movement using virtual planning for non-syndromic facial asymmetry cases—A systematic review», *Oral Maxillofac. Surg.* (2022) <https://doi.org/10.1007/s10006-022-01059-w> apr.
- [20] P. Alcañiz, et al., «Soft-tissue simulation for computational planning of orthognathic surgery», *J. Pers. Med.* 11 (2021) <https://doi.org/10.3390/jpm11100982> fasc. 10, Art. fasc. 10, ott.
- [21] D. Salazar, P.E. Rossouw, F. Javed, e D. Michelogiannakis, «Artificial intelligence for treatment planning and soft tissue outcome prediction of orthognathic treatment: a systematic review», *J. Orthod.* 51 (2) (2024) 107–119, <https://doi.org/10.1177/14653125231203743>, volfascgiu.
- [22] J. Zhu, Y. Yang, e H.M. Wong, «Development and accuracy of artificial intelligence-generated prediction of facial changes in orthodontic treatment: a scoping review», *J. Zhejiang Univ. Sci. B* 24 (11) (2023) 974–984, <https://doi.org/10.1631/jzus.202300244>, volfascnov.
- [23] H. Sankar, et al., «Role of artificial intelligence in treatment planning and outcome prediction of jaw corrective surgeries by using 3-D imaging: a systematic review», *Oral Surg. Oral Med. Oral Pathol. Oral Radiol* 139 (2025) 299–310, <https://doi.org/10.1016/j.oooo.2024.09.010>, volfasc. 3mar.
- [24] A.A. Almarhoumi, «Accuracy of artificial intelligence in predicting facial changes post-orthognathic surgery: a comprehensive scoping review», *J. Clin. Exp. Dent.* 16 (5) (2024) e624–e633, fasc.
- [25] M.F. Miragall, et al., «Face the future—Artificial intelligence in oral and maxillofacial surgery», *J. Clin. Med.* 12 (2023) <https://doi.org/10.3390/jcm12216843> volfasc. 21, Art. fasc. 21, gen.
- [26] R. Andlauer, et al., «3D-Guided face manipulation of 2D images for the prediction of post-operative outcome after cranio-maxillofacial surgery», *IEEE Trans. Image Process.* 30 (2021) 7349–7363.
- [27] G.R.J. Swennen, in: G. Swennen, A. c. di (Eds.), «3D Virtual Treatment Planning of Orthognathic Surgery», in *3D Virtual Treatment Planning of Orthognathic Surgery: A Step-By-Step Approach for Orthodontists and Surgeons*, Springer, Berlin, Heidelberg, 2017, pp. 217–277, https://doi.org/10.1007/978-3-662-47389-4_3.
- [28] R. ter Horst, et al., «Three-dimensional virtual planning in mandibular advancement surgery: soft tissue prediction based on deep learning», *J. Cranio-Maxillofac. Surg.* (2021) <https://doi.org/10.1016/j.jcms.2021.04.001> apr.
- [29] C. Tanikawa, e T. Yamashiro, «Development of novel artificial intelligence systems to predict facial morphology after orthognathic surgery and orthodontic treatment in Japanese patients», *Sci. Rep.* 11 (1) (2021) 15853 <https://doi.org/10.1038/s41598-021-95002-w> fascago.
- [30] L. Ma, et al., «Simulation of postoperative facial appearances via geometric deep learning for efficient orthognathic surgical planning», *IEEE Trans. Med. Imaging* 42 (2) (2023) 336–345, <https://doi.org/10.1109/TMI.2022.3180078>, volfascFeb.
- [31] W. Du, et al., «Postoperative facial prediction for mandibular defect based on surface mesh deformation», *J. Stomatol. Oral Maxillofac. Surg.* 125 (2024) 101973 <https://doi.org/10.1016/j.jormas.2024.101973> fasc. 5, Supplement Zott.
- [32] R. Ali, R. Lei, H. Shi, e J. Xu, «Cranio-maxillofacial post-operative face prediction by deep spatial multiband VGG-NET CNN», *Am. J. Transl. Res.* 14 (4) (2022) 2527–2539, fascapr.
- [33] I.-H. Kim, et al., «Orthognathic surgical planning using graph CNN with dual embedding module: external validations with multi-hospital datasets», *Comput. Methods Programs Biomed.* 242 (2023) 107853 <https://doi.org/10.1016/j.cmpb.2023.107853> voldic.
- [34] H. Xie, J. Song, Y. Zhong, J. Li, C. Gu, e K.-S. Choi, «Extended Kalman filter nonlinear finite element method for nonlinear soft tissue deformation», *Comput. Methods Programs Biomed.* 200 (2021) 105828 <https://doi.org/10.1016/j.cmpb.2020.105828> mar.
- [35] W. Hou, P.X. Liu, e M. Zheng, «A new model of soft tissue with constraints for interactive surgical simulation», *Comput. Methods Programs Biomed.* 175 (2019) 35–43, <https://doi.org/10.1016/j.cmpb.2019.03.018>, lug.
- [36] R.E. Woods, S.L. Eddins, e R.C. Gonzalez, «Digital image processing using MATLAB», 2009.
- [37] L. Ulrich, E. Vezzetti, S. Moos, e F. Marcolin, «Analysis of RGB-D camera technologies for supporting different facial usage scenarios», *Multimed. Tools Appl.* 79 (2020) 29375–29398, <https://doi.org/10.1007/s11042-020-09479-0>, fasc. 39ott.
- [38] L. Ulrich, et al., «Can ADAS distract driver's attention? An RGB-D camera and deep learning-based analysis», *Appl. Sci.* 11 (24) (2021) 11587 fasc.
- [39] G. Maculotti, et al., «A methodology for task-specific metrological characterization of low-cost 3D camera for face analysis», *Measurement* 200 (2022) 111643 <https://doi.org/10.1016/j.measurement.2022.111643> ago.
- [40] E.C. Olivetti, et al., «Three-dimensional evaluation of soft tissue malar modifications after zygomatic valgization osteotomy via geometrical descriptors», *J. Pers. Med.* 11 (2021) 205, <https://doi.org/10.3390/jpm11030205>, fasc. 3mar.
- [41] E. Vezzetti, e F. Marcolin, «3D human face description: landmarks measures and geometrical features», *Image Vis. Comput.* 30 (10) (2012) 698–712, <https://doi.org/10.1016/j.imavis.2012.02.007>, fascott.
- [42] E. Vezzetti, F. Marcolin, e G. Fracastoro, «3D face recognition: an automatic strategy based on geometrical descriptors and landmarks», *Robot. Auton. Syst.* 62 (12) (2014) 1768–1776, <https://doi.org/10.1016/j.robot.2014.07.009>, fascdic.
- [43] M.G. Violante, F. Marcolin, E. Vezzetti, L. Ulrich, G. Billia, e L. Di Grazia, «3D Facial expression recognition for defining users' Inner requirements—An emotional design case study», *Appl. Sci.* 9 (11) (2019) 2218, volfasc.
- [44] N. Meiyappan, S. Tamizharasi, K.P. Senthilkumar, e K. Janardhanan, «Natural head position: an overview», *J. Pharm. Bioallied Sci.* 7 (2015) S424–S427, <https://doi.org/10.4103/0975-7406.163488>, volfasc. Suppl 2ago.
- [45] T.-C. Hsung, W.-K. Yeung, W.-S. Choi, W.-K. Luk, Y.-Y. Cheng, e Y.-H. Lam, «Recording natural head position using cone beam computerized tomography», *Sensors* 21 (2021) <https://doi.org/10.3390/s21248189> volfasc. 24, Art. fasc. 24, gen.
- [46] M.S. Demétrio, D.A.A. Marlière, S. de, M. Barbosa, R.A. Pereira, e H.M. da Silveira, «Different modalities to record and transfer natural head position to virtual planning in orthognathic surgery: case reports of asymmetric patients», *J. Maxillofac. Oral Surg.* 20 (3) (2021) 443–454, <https://doi.org/10.1007/s12663-020-01376-1>, volfascset.
- [47] G.R.J. Swennen, F.A.C. Schutyser, e J.-E. Hausamen, *Three-Dimensional Cephalometry: A Color Atlas and Manual*, Springer Science & Business Media, 2005.
- [48] L. Ulrich, J.-L. Dugelay, E. Vezzetti, S. Moos, e F. Marcolin, «Perspective morphometric criteria for facial beauty and proportion assessment», *Appl. Sci.* 10 (1) (2020) <https://doi.org/10.3390/app10010008> fascp. 8, gen.
- [49] P.J. Besl e N.D. McKay, «Method for registration of 3-D shapes», in *Sensor Fusion IV: Control Paradigms and Data Structures*, SPIE, apr. 1992, pp. 586–606. doi:10.1117/12.57955.

- [50] Y. Chen, e G. Medioni, «Object modelling by registration of multiple range images», *Image Vis. Comput.* 10 (3) (1992) 145–155, vol fasc.
- [51] E. Vezzetti, F. Marcolin, S. Tornincasa, L. Ulrich, e N. Dagnes, «3D geometry-based automatic landmark localization in presence of facial occlusions», *Multimed. Tools Appl.* 77 (11) (2018) 14177–14205, <https://doi.org/10.1007/s11042-017-5025-y>, vol fasc giu.
- [52] X. Fan, Q. Jia, K. Huyan, X. Gu, e Z. Luo, «3D facial landmark localization using texture regression via conformal mapping», *Pattern Recognit. Lett.* 83 (2016) 395–402, <https://doi.org/10.1016/j.patrec.2016.07.005>, nov.
- [53] J. Lei, X. You, e M. Abdel-Mottaleb, «Automatic ear landmark localization, segmentation, and pose classification in range images», *IEEE Trans. Syst. Man Cybern. Syst.* 46 (2) (2016) 165–176, <https://doi.org/10.1109/TSMC.2015.2452892>, fasc feb.
- [54] J.M.H. Noothout, et al., «Deep learning-based regression and classification for automatic landmark localization in medical images», *IEEE Trans. Med. Imaging* 39 (2020) 4011–4022, <https://doi.org/10.1109/TMI.2020.3009002>, fasc. 12, ppdic.
- [55] E.C. Olivetti, et al., «Do facial soft tissue thicknesses change after surgeries correcting dental malocclusions? An intra- and inter-patient statistical analysis on soft-tissue thicknesses in BSSO + LFI surgeries», *Clin. Oral Investig.* 27 (9) (2023) 5049–5062, <https://doi.org/10.1007/s00784-023-05124-w>, fasc set.
- [56] H.-Y. Suh, H.-J. Lee, Y.-S. Lee, S.-H. Eo, R.E. Donatelli, e S.-J. Lee, «Predicting soft tissue changes after orthognathic surgery: the sparse partial least squares method», *Angle Orthod* 89 (6) (2019) 910–916, <https://doi.org/10.2319/120518-851.1>, vol fasc mag.